RC22859 (W0307-185) July 29, 2003
Materials Science

IBM Research Report

Hardmask Technology for Sub-100 nm Lithographic Imaging

Katherina Babich, Arpan P. Mahorowala, David R. Medeiros, Karen Petrillo, Marie Angelopoulos, Alfred Grill, Vish Patel
IBM T. J. Watson Research Center
Route 134, Yorktown Heights, NY 10598

Scott Halle, Timothy A. Brunner, Richard Conti, Scott Allen, Richard Wise
IBM SRDC, 1580 Route 52,
Hopewell Junction, NY 12533

Research Division
Almaden - Austin - Beijing - Delhi - Haifa - India - T. J. Watson - Tokyo - Zurich

LIMITED DISTRIBUTION NOTICE: This report has been submitted for publication outside of IBM and will probably be copyrighted if accepted for publication. It has been issued as a Research Report for early dissemination of its contents. In view of the transfer of copyright to the outside publisher, its distribution outside of IBM prior to publication should be limited to peer communications and specific requests. After outside publication, requests should be filled only by reprints or legally obtained copies of the article (e.g. , payment of royalties). Copies may be requested from IBM T. J. Watson Research Center ,
P. O. Box 218, Yorktown Heights, NY 10598 USA (email: reports@us.ibm.com). Some reports are available on the internet at http://domino.watson.ibm.com/library/CyberDig.nsf/home .

Hardmask technology for sub-100 nm lithographic imaging

Katherina Babich, Arpan P. Mahorowala, David R. Medeiros, Karen Petrillo, Marie Angelopoulos, Alfred Grill, Vish Patel
(IBM T. J. Watson Research Center, Route 134, Yorktown Heights, NY 10598)

Scott Halle, Timothy A. Brunner, Richard Conti, Scott Allen, Richard Wise
(IBM SRDC, 1580 Route 52, Hopewell Junction, NY 12533)

ABSTRACT

We have developed a silicon-based, plasma-enhanced chemical vapor deposition (PECVD) prepared material that performs both as an antireflective coating (ARC) and a hardmask and thus enables the use of thin resists for device fabrication. This ARC/hardmask material offers several advantages over organic bottom antireflective coatings (BARC). These benefits include excellent tunability of the material's optical properties, which allows superior substrate reflectivity control, and high etch selectivity to resist, exceeding 2:1. In addition, this material can serve as an effective hardmask etch barrier during the plasma etching of dielectric stacks, as the underlying silicon oxide etches eight times faster than this material in typical fluorocarbon plasma. These properties enable the pattering of features in 1-2μm dielectric stacks using thin resists, imaging that would otherwise be impossible with conventional processing. Lithographic performance and etch characteristics of a thin resist process over both single layer and index-graded ARC/hardmask materials will be shown.

Keywords: Antireflective coatings, hardmasks, combined ARC/hardmask materials, PECVD ARCs, index graded ARCs, optical constants, high resolution lithography, thin resist process, image collapse, adhesion failure

1. INTRODUCTION

Thin resists are needed for high resolution lithography; but as we enter the era of sub-100nm imaging, the use of the term 'resist' in the sense of a material that provides masking or protective properties may become inappropriate. Resists have been used as etch masks to transfer patterns into underlying semiconductor materials, but thin polymer films may not be able to carry this function with much effectiveness. Resist thickness has continued to decrease with each new product generation to facilitate improved process latitude, especially when coupled with optical tools with high numerical aperture (NA). Figure 1 shows the thickness of the resist as a function of feature size having the conventional 3-3.5 to 1 aspect ratio, a value above which the mechanical instability of the images results in image collapse.[1, 2] For example, according to semiconductor industry association (SIA) road map, resists of ~500-600 nm thickness have been used for KrF (248nm) lithography to meet the patterning requirements of 150-135nm device technologies. ArF (193nm) lithography is being implemented for the 120-110nm technologies with typical 193nm photoresist films of ~300-350nm. Resist thickness is expected to continue to decrease even more dramatically as optical absorbance issues become very significant for post-193nm technologies such a F_2 (157nm) and EUV lithography. Resist films are currently projected to be less than 200nm and potentially less than 100nm depending on the particular resist chemistry, for these applications. [3, 4]
As it has been necessary to reduce resist thickness to accommodate higher resolution imaging, the dry etch resistance of resist materials has largely remained the same or, in some cases has decreased.[5] The net result is that there is insufficient resist thickness to allow effective image transfer to the underlying substrate. Additionally, significant resist loss occurs during the reactive ion etch open process of the ARC. Further diminishing the "resistive" properties of the resist, current organic BARC materials have less than 1:1 etch selectivity to resist. Thus, about 100nm of the resist is consumed during ARC open, as illustrated in Figure 1. With high-resolution imaging, this becomes a fundamental process limitation. For example, at 100nm ground rules, a nominal resist thickness of 350nm affords an effective thickness of 250nm after the ARC open process. This thickness is insufficient to provide an adequate etch mask for image transfer to the underlying substrate. Thus, a paradox results in that a thin resist is desirable for imaging while a thicker resist is needed for etch

transfer. New imaging schemes decoupling lithographic performance and etch resistance are required for next generation device fabrication.

The thin resist process described in this manuscript is enabled by the use of a novel antireflective coating with build-in hardmask properties that provides a significant enhancement of etch selectivity to resist and substrate materials: > 2:1 to resist and > 10:1 to oxide. It has been shown that the optical properties of this novel ARC/hardmask are tunable over a wide range and that these materials are compatible with conventional 248nm, 193nm, and electron beam single layer resist systems. This research has resulted in a process combining a thin resist on the ARC/hardmask that can be used to transfer high resolution images into 1.2-1.8μm thick oxide substrates. Dense images, as small as 50nm, generated by electron beam lithography were transferred into 300nm silicon dioxide layer by using this process.

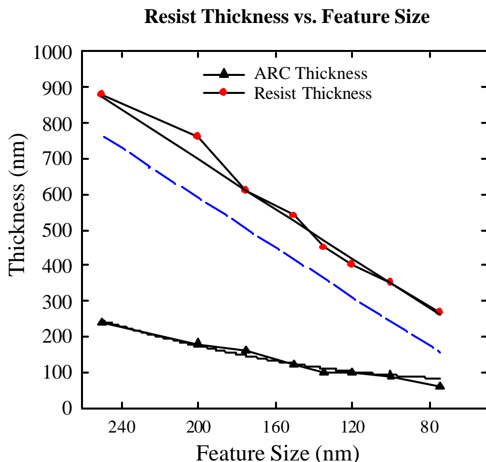

Figure 1. Graph comparing projected resist thickness as a function of feature size (circles) to that of corresponding ARC thickness (triangles). The dashed line represents the 'effective' resist thickness, which takes into account the resist thickness lost during ARC-open plasma etch

2. EXPERIMENTAL

The imaging resists used in this study included Shipley UV-82 for 248nm lithography, Sumitomo PAR-710 and PAR-715 for 193nm lithography, and IBM's internally developed KRS-XE resist for electron beam lithography. ARC/Hardmask materials were deposited in an internally built parallel plate radio frequency (rf) plasma enhanced chemical vapor deposition (PECVD) reactor using a 13.56 MHz rf power supply or on a commercial PECVD platform using a precursor mixture containing silicon species. The thickness of the imaging resist varied from 110nm to 400nm. Imaging at 248nm was carried out on 0.63NA ASML500 stepper using an attenuated phase shift mask (APSM). 193nm lithography was performed on either a 0.63NA Nikon or 0.75NA ASML5000 steppers using both attenuated and alternating phased shift masks. A Leica direct-write tool operating at an accelerating voltage of 100 keV was used for the electron beam patterning.

The photoresist image transfer into the ARC/hardmask material was carried out either on a high-density plasma etcher using a Cl_2-based chemistry or on a medium density etcher using polymerizing fluorocarbon based chemistry. The hard mask properties of the ARC/hardmask material were evaluated while etching borosilicate glass (BSG) on a medium density etcher using a non-polymerizing fluorocarbon-based etch chemistry.

The optical constants, index of refraction *(n)* and extinction coefficient *(k)*, at 193nm and 248nm of the imaging resists and various ARCs and ARC/hardmask materials were measured by two independent techniques. Variable Angle Spectroscopic Ellipsometry (VASE) was carried on a Woollam WVASE32 instrument operating in 146-1100nm wavelength range. Reflectmetry with subsequent n&k determination was performed using an n&k 1200 Analyzer from n&k Technology.

3. Antireflective properties of ARC/Hardmask material

3.1 Theoretical Aspects of ARC Optimization

The combined ARC/hardmask concept is a new imaging scheme that decouples lithography and pattern transfer and offers considerable leverage for thin resist processing. By providing both effective ARC properties and enhanced etch selectivity to resist comparable features may be etched into the substrate using thinner resists. Alternatively, for the same resist thickness used in a conventional single layer resist (SLR) with ARC process, deeper features may be patterned into the substrate by the addition of this material. Various ARC/hardmask schemes are possible, depending on the integration needs.

As previously discussed, efficient antireflective properties are among the critical requirements of ARC/hardmask materials. In order to reduce substrate reflectivity variations and improve critical dimension (CD) control, the swing ratio or amplitude has to be minimized. The swing ratio, S, is defined as:

$$S = 4(R_1R_2)^{0.5}e^{-\alpha d} \qquad (\mathbf{1})$$

where, in Equation **1**, R_1 is the reflectivity at the resist air interface, R_2 is the reflectivity at the resist substrate interface, α is the absorption coefficient of the resist, d is the resist thickness.[6] The absorption coefficient is defined in Equation **2**, where k is the extinction coefficient and λ is the optical wavelength.

$$\alpha = 4\pi k/\lambda \qquad (\mathbf{2})$$

In an ARC/hardmask scheme, the swing ratio is reduced by minimizing R_2. This is accomplished by optimization of the complex refractive index and film thickness at the ARC/resist interface using simulation. Computations are based on algorithms that use the Fresnel coefficients.[7]

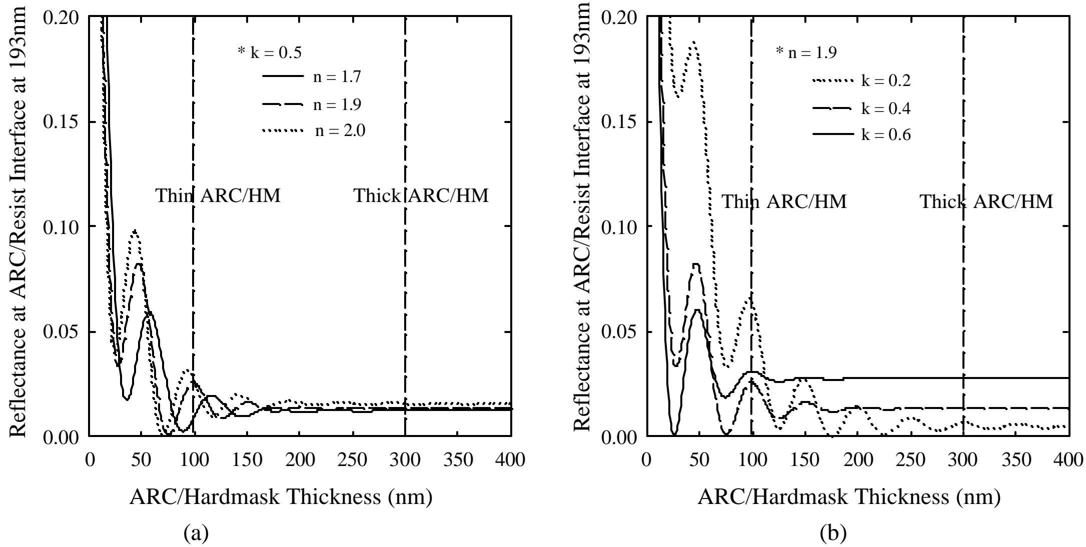

Figure 2. Reflectance at the ARC/resist interface at 193nm for (a) different *n* values of the ARC/hardmask material while maintaining *k* constant and (b) for different *k* values while keeping *n* fixed.

The simulated structure comprises a Si substrate, an ARC/hardmask layer and the imaging photoresist. The acrylate-based 193nm resist used in this study has n=1.72 and k=0.018 at 193nm. The reflectance at the ARC/resist interface of thin ARCs of ~100nm exhibits alternating maxima and minima, the positions of which depend on the n and k of the ARC/hardmask film. Figure 2a shows the reflectance at the ARC/resist interface at 193nm as a function of

ARC/hardmask thickness for different values of n while keeping k constant at 0.5. High values of n and k, on the order of 2.0-2.1 and 0.5-0.6 respectively, are desirable for thin ARCs in order to minimize the thickness at the second minimum. While thin absorbing ARCs, operating at a reflectance minimum, can significantly suppress the reflectivity for a particular substrate; they are not as effective if the substrate thickness varies, or if there is significant topography on the wafer. Conversely, thick ARCs of ~300nm, can provide better reflectivity control due to the small variation in reflectance caused by substrate reflectivity changes. Figure 2b shows the reflectivity at the ARC/resist interface at 193nm versus ARC thickness for different k values while keeping the value of n fixed. In this case, the extinction coefficient has a stronger impact on reflectance versus that of the index of refraction. The ARC film with n values in the range of 1.70 to 1.95 and k of ~0.20 to 0.22 will provide minimal thin film interference at this interface.

3.2 Optical properties of Si based ARC/hardmask materials

The optical constants of the Si based PECVD deposited ARC/hardmask materials were tuned by altering precursor composition and plasma polymerizing conditions such as substrate temperature, deposition power, pressure and flow rates. It was found that nature of the precursors as well as the substrate temperature and deposition power have the strongest impact on the optical properties of the de posited films. Conversely, the operating pressure and gas flow rates are relatively less important. Figures 3a and 3b show the variation of n at 248nm of the deposited films as a function of deposition bias and substrate temperature, respectively.

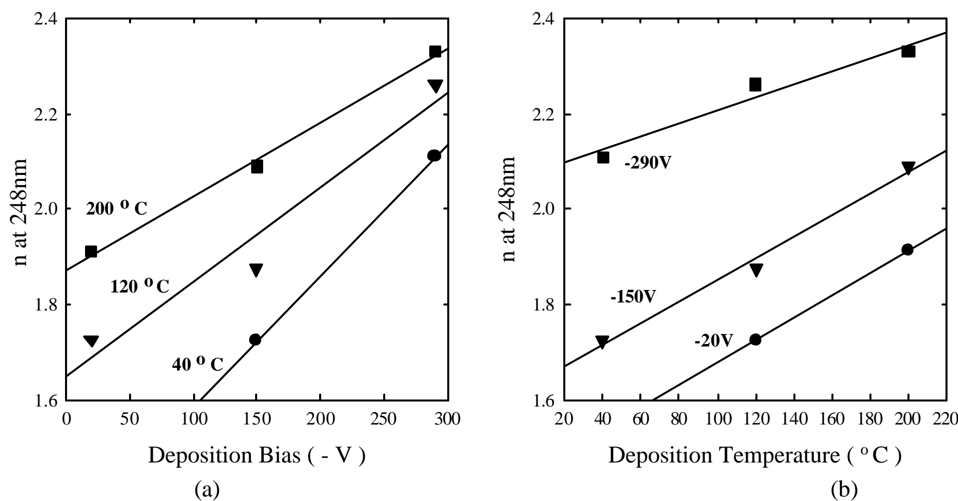

Figure 3. Variation of *n* at 248nm of ARC/hardmask PECVD films as a function of deposition bias at three different temperatures (a) and as a function of substrate temperature at three different biases (b).

Tool	Conditions	n_{193nm}	k_{193nm}	n_{248nm}	k_{248nm}
In-house	1	1.750	0.043	1.592	0.005
In-house	2	1.853	0.288	1.764	0.074
In-house	3	1.963	0.464	2.084	0.301
In-house	4	2.004	0.646	1.958	0.456
Commercial	5	1.615	0.045	1.512	0.007
Commercial	6	1.790	0.155	1.728	0.033
Commercial	7	1.971	0.370	1.924	0.215
Commercial	8	2.264	0.645	2.315	0.544

Table I. Variation of n and k at 193nm and 248nm of ARC/hardmask PECVD films deposited on two different reactors at various plasma polymerization conditions showing the tunability of the antireflective properties of these materials.

Table 1 shows the tunability of optical constants of ARC/hardmask materials at 193nm and 248nm for various precursor chemistries and plasma polymerization conditions. For example, by varying the deposition conditions the n at 193 can be varied from ~1.62 to ~2.26, with a corresponding range of k at this wavelength of ~0.045 to ~0.65. Similarly, at 248 nm, n can vary from ~1.51 to ~2.31 with k values of ~0.007 to ~0.54. The well-characterized optical tunability of the films allows fine-tuning of the ARC/hardmask film for specific applications. Such flexibility is generally not available when using spin-on ARCs. It should be noted that the ARC/hardmask films deposited for 248nm and 193nm lithography differ compositionally.

3.3 Index graded ARCs

Employing graded index ARC films can further reduce the reflectance at the ARC/resist interface and the swing ratio.[8-10] PECVD deposition is amenable to forming graded ARCs because the optical properties can be fine-tuned by continuously varying the deposition conditions, thereby creating a gradient in optical properties throughout the thickness of the film. When the refractive index and extinction coefficient of the ARC top and bottom surfaces perfectly match those of their adjacent layers, zero reflection at the resist/ARC interface can be achieved. The use of graded index ARCs can negate the effect of topography and substrate thickness variation, thereby further assisting with CD control. The simulated reflectivity curves for a 193nm lithography scheme in Figure 4 show that the reflectance at the resist/hardmask interface can be reduced to almost zero by using such a graded ARC/hardmask approach with n=2.1 and k=0.7 at the bottom and n=2.0 and k=0.2 on a top and bottom layer of >100nm thickness and top layer thickness ~. Such a low level of reflectivity is unattainable with single layer ARC materials.

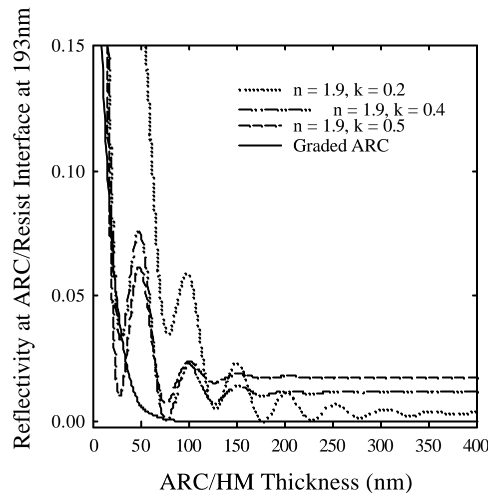

Figure 4. Simulated reflectance at 193nm at the resist/ARC interface for various ARC/hardmask thicknesses. The top four curves were generated varying *k* from 0.2 to 0.5 while keeping *n* constant at 1.9. The lowermost curve, generated for a graded ARC/hardmask layer, suggests near complete suppression of reflectance by the graded ARC/hardmask film when the thickness is >100nm.

3.4 Reflectivity Effects for High NA Imaging or ARC's requirements for high NA lithography

The demand for high-resolution imaging dictates the use of exposure tools with NA of 0.85 or even higher. Interesting optical effects occur with very high NA imaging driven by the fact that images in a resist are formed by oblique waves close to Brewster's angle, where the two polarization components with their electric field vectors oriented in the x- and y-direction, commonly referred to as transverse magnetic (TM) and transverse electric (TE) respectively, are not transmitted

equally. The implications of this optical effect on lithographic processes were described in detail by Brunner, et al.[22] One of the discussion topics in this paper was the effect of TE and TM reflectivity over a full range of angles in conjunction with high NA imaging as well as the consequences on ARC performance and swing curve effects. The authors showed that ordinary single layer ARCs, currently used in manufacturing, can provide low reflectivity at normal incidence, whereas at higher incidence, reflectivity increases significantly for both TE and TM. Furthermore, a significant difference between TE and TM emerges as the angle of incidence becomes more oblique. An index graded ARC, as described in previously, with n=2.1 and k=0.7 at the bottom and n=2.0 and k=0.2 on a top can provide low reflectivity over the full range of angles. Figure 5 shows the reflectance at the ARC/resist interface as a function of sin(θ) in air for both single layer ARC and index graded ARC at oblique angles. One of the additional benefits of the graded Si based ARC/hardmask materials is their capability to provide enhanced reflectivity control for high NA lithography.

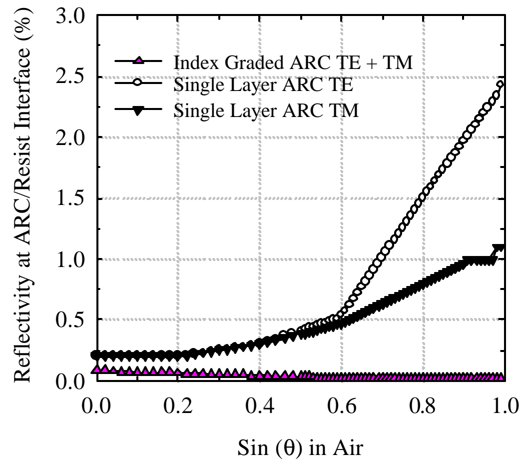

Figure 5. Simulated reflectance at the resist/ARC interface for single layer ARC and index graded ARC as a function of sin(θ)

4. Lithographic Properties of Si based ARC/hardmask materials

Compatibility with various resists is another critical requirement of ARC/HM materials. Chemical interactions at the ARC/resist interface have been reported during the evaluation of other PECVD ARCs such as SiON, TiN and CrON.[12-14] The basic nature of these ARCs has been attributed as the cause some profile imperfections, commonly called 'footing', a defect which significantly impedes implementation of these materials to manufacturing.

High quality lithography was demonstrated on both graded and single layer Si based PECVD deposited ARC/hardmask materials using a wide variety of 248nm, 193nm and electron beam resists. That is, no footing, undercut or residue was observed during patterning. Figure 5 shows SEM images of 150nm line and space (L/S) patterns of UV0-82 resist obtained using 248nm lithography (5a); 120nm L/S patterns of PAR-710 resist obtained using 193nm lithography (5b); and 100nm L/S patterns of KRS-XE resist using electron beam lithography (5c). It should be noted that the surface of Si based ARC/hardmask materials were specifically tailored to prevent resist footing.

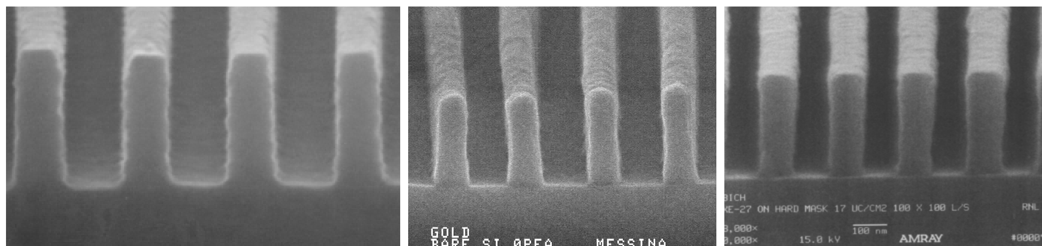

(a) (b) (c)

Figure 6. SEM images of high resolution half-pitch line-and-space structures patterned on tuned ARC/hardmasks using UV82 at 248 nm giving 150 nm resolution (a); PAR-710 at 193 nm giving 120 nm resolution (b); and KRS-XE with electron beam lithography giving 100 nm resolution (c).

5. Etch characteristics of Si based ARC/HM materials

Having the appropriate etch selectivity to both resists and to dielectric materials such as SiO_2 is among the most challenging requirements of ARC/HM materials. Current organic ARCs have elemental chemical composition very similar to photoresists. This leads to little differentiation between the etch characteristics of these two material sets, resulting in a significant portion of the resist being consumed during the ARC open process. Thus, less resist remains for substrate etching. Furthermore, the organic ARC offers minimal etch-resistance during subsequent dielectric etch. For high-resolution lithography it is important to design ARC materials that will provide good etch selectivity to resist as well as provide hardmask characteristics for the subsequent etch transfer.

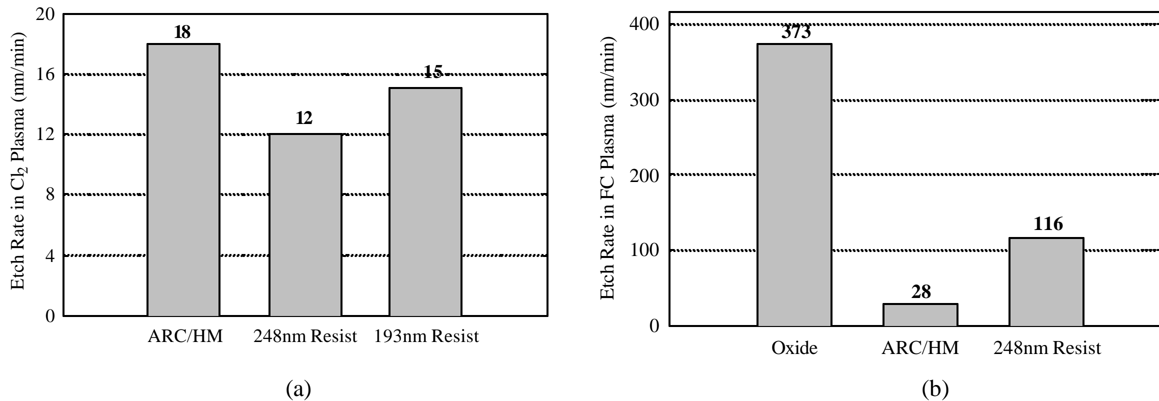

Figure 7. Blanket etch rates of ARC/hardmask and two photoresists in a Cl_2-based plasma (a) and of ARC/hardmask, oxide and a 248nm photoresist in a non-polymerizing fluorocarbon-based plasma (b).

Figure 7a shows the blanket etch rates of a Si based ARC/hardmask compared with those of resist films in a Cl_2-based chemistry on a high-density plasma etch tool. The blanket selectivities of ARC/hardmask to resist of ~ 1.5:1 mprove to ~2:1 during patterned etches. This selectivity of 2:1 compares very favorably with the selectivity values of organic ARC to resist of ~0.7. Assuming the post-developed resist thickness to be ~350nm and an ~100nm thick ARC, the post ARC-open, effective resist thickness would be ~300nm using the ARC/hardmask scheme versus ~210nm using organic ARC – an increase of over 40-%. ARC/hardmask materials have also shown efficient etch-resistance in fluorocarbon-based chemistries used to etch silicon oxide. Figure 7b compares the blanket etch rate of silicon oxide versus ARC/hardmask and a PHS-based 248nm resist in a non-polymerizing fluorocarbon-based chemistry, etched on a medium density plasma tool. The ARC/hardmask etches significantly slower than resist and therefore should provide a better mask for oxide etching. The measured blanket etch selectivity between oxide and ARC/hardmask actually exceeds 13:1. In addition, during patterned etches (*vide infra*), the ARC/hardmask materials have shown little propensity to facet as compared with resist. Additionally, an etch selectivity of 2.5:1 for ARC/hardmask material to resist in a highly polymerizing fluorocarbon-based chemistry on a medium density plasma etcher was also demonstrated.

Pattern transfer using an ARC/hardmask material for 248nm lithography is demonstrated in Figure 8. First, 150nm L/S features in 340nm thick UV-82 resist were patterned as shown in Figure 8a. The resist images were then transfer into 300nm thick ARC/hardmask material using the high-density plasma with a Cl_2-based chemistry, as shown in 8b. The resist was subsequently striped using O_2 plasma, as in 8c, resulting in high quality images with vertical profiles. The 300nm thick ARC/hardmask material was then used as mask to transfer the patters into 300nm thick SiO_2, shown in 8d. No

ARC/hardmask thickness loss was observed during this process, indicating selectivity to oxide in excess of 10 to 1. Only minor corner faceting was observed, which has been attributed to energetic ion bombardment.

The feasibility of using ARC/hardmask approach for 193nm lithography was demonstrated in combination with fluorocarbon-based etch transfer process. 120nm contacts were printed in ~350nm thick PAR-710 resist over graded ARC/hardmask with tuned n and k values to afford the minimal reflectance at ARC/resist interface as shown in Figure 9a. The resist images were then transferred into ~450nm thick ARC/hardmask material using a fluorocarbon-based chemistry, as shown in Figure 9b.

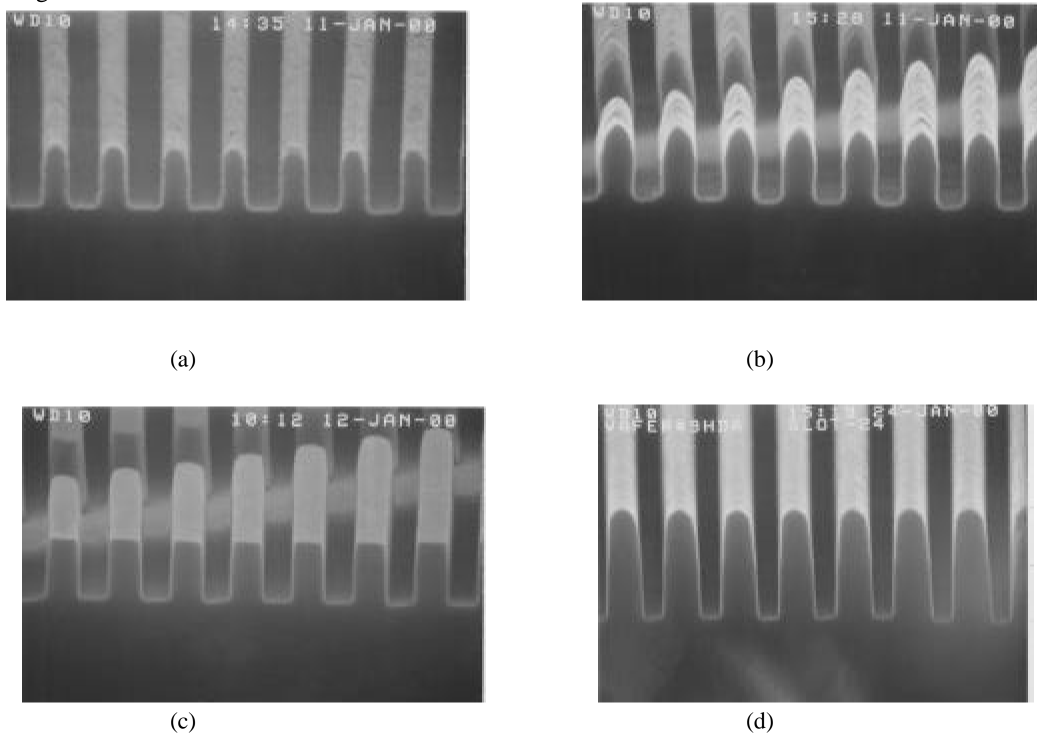

(a) (b)

(c) (d)

Figure 8. SEM images of 150nm L/S patters in UV-82 resist obtained using 248nm lithography (a); transfer of image into 300nm thick ARC/hardmask with Cl_2-based plasma (b); post-resist strip (c); and pattern transfer into 300nm thick SiO_2 with fluorocarbon plasma (d).

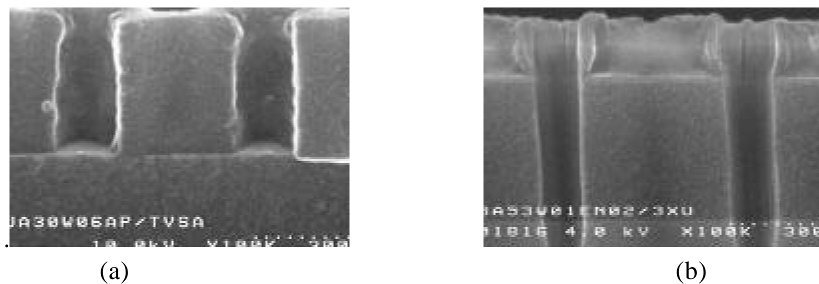

(a) (b)

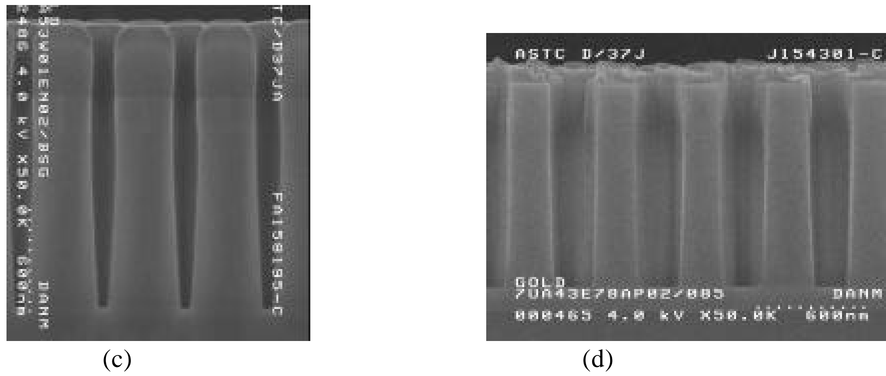

(c) (d)

Figure 9. SEM images of 120nm contact patterns in PAR-710 resist (a), ARC/hardmask open process in fluorocarbon-based plasma chemistry (b), pattern transfer into 1.2µm thick BSG layer using ARC/HM approach (c), conventional SLR/BARC scheme (d)

Due to the significant passivation that accompanies the etch process, even higher ARC-to-resist selectivities (>2.5 compared to ~2 for the Cl_2-based process) and faster etch rates (~450nm/min compared to ~200nm/min for the Cl_2-based process) were achieved.

Using the combination of resist with ARC/hardmask material as an etch mask, patterns were then transferred into dielectric stack. A significant portion of ARC/hardmask material remains after pattern transfer into 1.2µm thick borosilicate glass (BSG), as shown in Figure 9c. This demonstrates that either deeper BSG stacks can be etched or that the ARC/hardmask thickness can be decreased. In contrast, when a single layer of PAR-710 (~350nm) over 90nm of organic ARC was used to pattern a 1.2µm BSG, very little resist remains after the pattern transfer, as in Figure 9d. The contrast between these two schemes shows the limited extensibility of the SLR approach for future device manufacturing. SEM images corresponding at intermediate stages of the etch process suggest that ARC/hardmask-to-BSG selectivity of >10 greatly exceeds the SLR/BARC-to-BSG selectivity of ~ 4-5.

7. Examples of device level processing

The deep trench (DT), or trench capacitor level, traditionally has required thick resist due to the challenge associated with etching through a thick dielectric stack.[15] As device dimensions shrink, it is necessary to form deeper trenches to maintain device performance. This in turn necessitates thicker BSG masks. It is becoming increasingly difficult to pattern such thick BSG masks using SLR processes in conjunction with organic ARCs. The application of the ARC/hardmask approach to print very high aspect ratio resist features at smaller dimensions alleviates this problem. Figure 10a shows patterning of the DT dielectric stack consisting of 1.8µm BSG over silicon nitride, Si_3N_4, layer using the integration scheme described in Figure 9, but with a thinner ARC/hardmask of ~250nm. Figure 10b shows 90nm contacts etched into 1.5µm BSG using Si based ARC/HM material. Forming similar patterns in 1.8µm BSG layer with the conventional SLR was not possible.

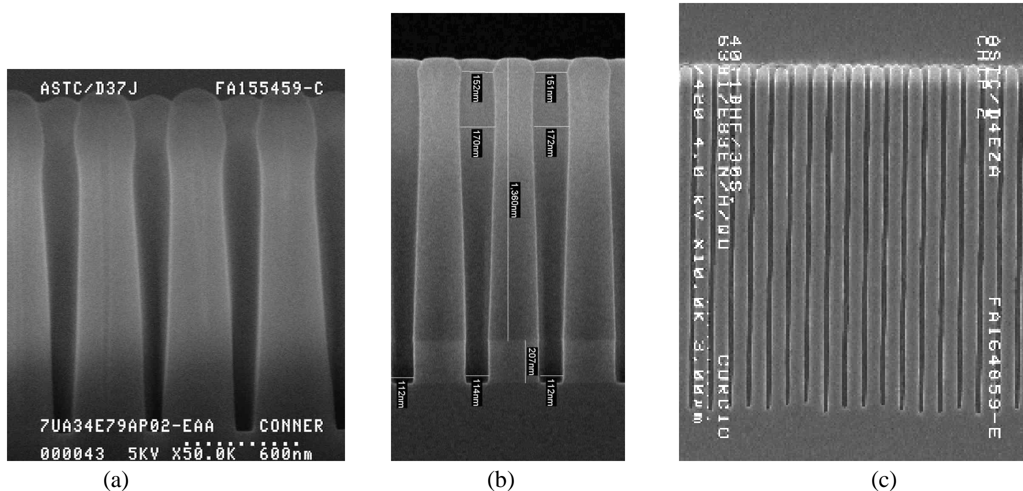

(a) (b) (c)

Figure 10. Pattern transfer into 1.8 µm thick BSG layer using ~250nm thick ARC/HM (a), 90nm DT patterns etched into 1.5 µm thick BSG layer. Cross sectional images of 8 µm (c) deep silicon trenches obtained by using ARC/HM approach

After the BSG/Si_3N_4 etch, the next step in DT patterning involves transfer of the deep trenches into the underlying silicon. Figure 10c shows the cross-sectional SEM images of ~8µm DT's etched into Si using the ARC/hardmask approach. An ultra-high aspect ratio of greater than 65:1 at feature sizes of 120nm was attained with this technology.

Some additional benefits of the ARC/hardmask approach were observed during DT patterning. As previously reported, insufficient resist thickness during etch transfer can lead to significant surface roughening and the formation of undesirable artifacts such as substrate 'microcrevicing', as shown in Figure 11A[16]. PECVD deposited ARC/hardmask materials are highly crosslinked covalent networks and therefore are substantially denser then polymer films [17]. The use of these materials as ARC/hardmasks can potentially prevent or minimize the transfer of the resist roughness into substrate materials, as is illustrated in Figure 11B, where no microcrevicing was observed in the 135nm contacts etched into Si_3N_4 by this approach.

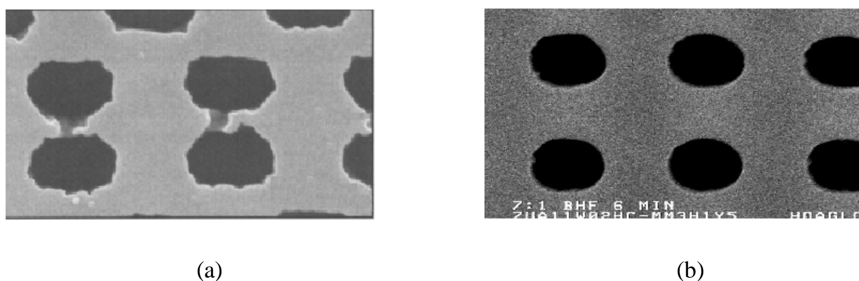

(a) (b)

Figure 11. Top down scanning electron micrograph showing microcrevicing around contact holes on a dielectric substrate after etch (a). In contrast, no microfissures observed on 135nm contacts etched into silicon nitride using ARC/HM process.

8. Sub-100nm Patterning and Image Collapse

Sub-100nm pattering has imposed increasingly stringent requirements on resist performance. Major resist requirements include high resolution, excellent process window, sufficient etch resistance and collapse free process. It was previously discussed that image collapse issues could be a limiting factor in SLR imaging for sub-100 nm nodes.[1, 2] There are many different mechanisms associated with pattern collapse addressed in the literature: bending[1, 2, 18], mechanical failure [19], line "pinching", resist peeling from the substrate or delamination[20]. This study focuses only on the

later scenario and examines the issues of image collapse driven by adhesion failure influenced by substrate and its implications on ARC design. This simplified case may be described by the balance of two competing forces: capillary and adhesive. Image collapse occurs naturally during photoresist development/drying process due the surface tension of the rinse liquid resulting in capillary forces acting on resist walls [1, 2, 18]. Capillary forces described by Laplace equation:

$$F = \frac{\gamma}{r} \qquad (3)$$

where, in Equation **3**, γ is the surface tension of the rinse liquid, r is the radius of curvature of a spacing between lines. Image collapse can be dramatically influenced by substrate effects either preventing or promoting it depending on depending on adhesive properties of the substrate. Adhesive forces between photoresist and substrate are related to work of adhesion, W_{Adh} :

$$W_{Adh} = \gamma_V + \gamma_V - 2\gamma_2 \qquad (4)$$

where in Equation **4**, γ_V is the surface energy of substrate, γ_V is surface energy of resist, $2\gamma_2$ is the interfacial energy of substrate and resist.

If adhesive forces are greater then capillary forces, good adhesion strength between resist and substrate, e.g. ARC material is observed – allowing images to stand. When adhesion between resist and ARC is poor, capillary forces dominate resulting in resist adhesion loss with subsequent pattern collapse. Adhesion loss can be significantly suppressed by increasing adhesive forces, e.g. work of adhesion. As shown in Equation 4, W_{Adh} can be increased by increasing the surface energy of ARC material. We have found that surface properties such as surface energy (SE) and water contact angle (CA) of Si based PECVD deposited ARC/hardmask can be modified by various post plasma treatments. For example, the nature of the surface can be changed from highly hydrophilic with CA below 10 degrees to highly hydrophobic with CA equal or above 90 degrees. Surface energy was calculated using a harmonic model[21] with contact angle data from the following solvents: water, diiodomethane, formamide and xylene. Table 2 shows water contact angle, total surface energy and the polar component of surface energy for organic ARC and Si based ARC/hardmask with different surface treatments. The polar component of the surface energy is more closely related to the nature of the material as it is a measure of the surface energy associated with polar bonding (e.g. hydrogen bonds, dipole-dipole interactions); while dispersive energy is related to weaker 'nonpolar' interactions such as van der Waals forces. This analytical characterization data is in agreement with lithographic data described below (*vide infra*). Thus, it appears that strong bonding components dictate the differences between these surfaces and in turn the ability for high aspect ratio patterns to avoid adhesion failure. This allows a powerful tool and potential predictive capability for tailoring substrates to allow for enhanced process latitude.

Dense half-pitch features consisting of 90nm and 80nm L/S were printed in ~230nm thick PAR-715 using a 0.75 NA ASML 5000 stepper with a partial coherence of σ=0.4 exposures and an alt-PSM. In this experiment, two substrates were compared: AR-19 ARC from Shipley and graded Si ARC/hardmask. Figure 12 shows the comparison of depth of focus (DOF) latitude for 90nm equal L/S patterns printed over these substrates. In the case of AR-19, an increased sensitivity to pattern collapse was observed, even with resist aspect ratio below 3. Line collapse was observed at both -0.2 to +0.2µm focus. In contrast, no image collapse was observed on Si based ARC/hardmask for DOF between -0.2 to +0.3µm.

Substrate	Water Contact Angle (deg)	Surface Treatment	Total Surface Energy (dynes/cm)	Polar Component of Surface Energy (dynes/cm)
Organic ARC	50-65	-	42.4	12
Si based ARC/HM	10-12	Hydrophilic	-	-
Si based ARC/HM	72-77	Mixed	38.7	13
Si based ARC/HM	85-90	Hydrophobic	54.1	21

Table 2. Table 2 shows water contact angle, total surface energy and the polar component of surface energy for organic ARC and Si based ARC/hardmask with different surface treatments.

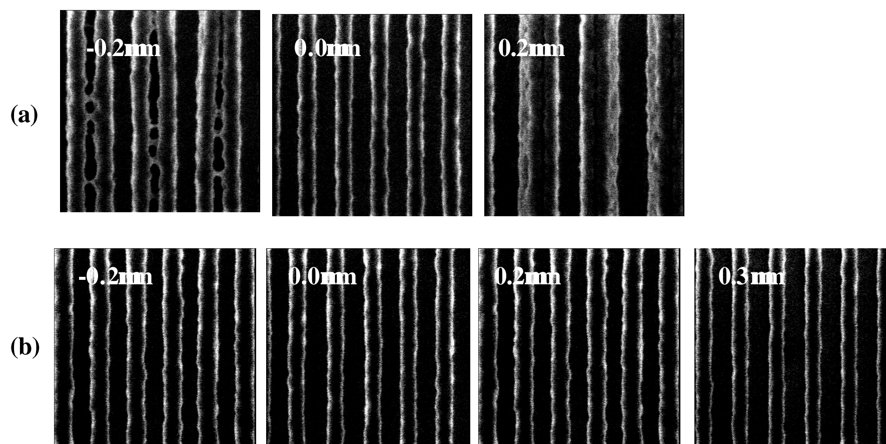

Figure 12. SEM images of high resolution half-pitch line-and-space structures patterned over organic ARC (a); over Si based ARC/HM material with highly hydrophobic surface (b) as a function of depth of focus.

For 80nm half-pitch line-and-space patterning, no image collapse and sufficient resist process window were observed for patterns printed over Si based ARC/hardmask. (Figure 13a). The process window was largely limited by the illumination conditions and resist performance and not by substrate-influenced image collapse. Conversely, complete line collapse, apparently driven by adhesion failure as shown in Figure 13(b), was observed for 80 nm equal L/S patterns over organic ARC material resulting in no process latitude with the conventional SLR/ARC approach. It should be noted that this complete lack of process latitude for this feature size may possibly be attributable to this particular resist/ARC combination. Presently, new organic ARC materials with improved adhesion characteristics capable of resolving 80nm images are under development by various commercial vendors. We have shown that ARC materials have substantial impact on resist process window, and surface properties of these materials can be tailored to enable a high resolution process.

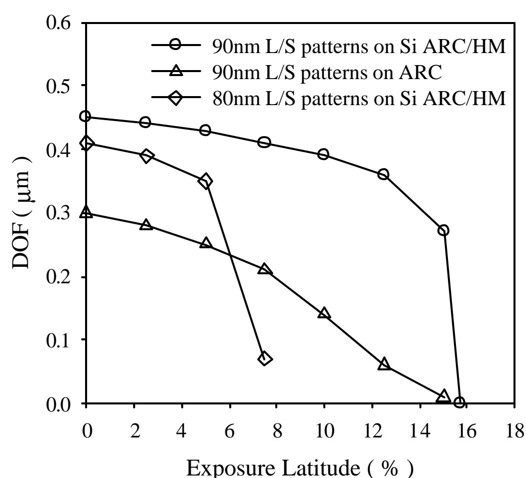

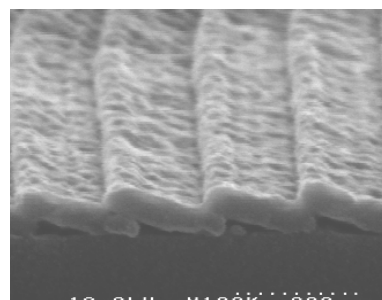

Figure 13. Process window comparison for half-pitch 80 and 90nm line-and-space structures patterned over organic ARC and Si based ARC/HM material (a), complete line collapse driven by adhesion failure for 80 nm half-pitch line-and-space patterns over organic ARC material (b)

9. ARC/HM technology for high resolution, thin resist processing

To demonstrate the extendibility of this technology to feature sizes below 100nm, electron beam lithography was employed. Electron beam patterning of KRS-XE, a chemically amplified resist designed especially for photomask manufacturing, on ARC/hardmask coated silicon wafers was achieved using a Leica direct write patterning tool operating at an accelerating voltage of 100 kV.

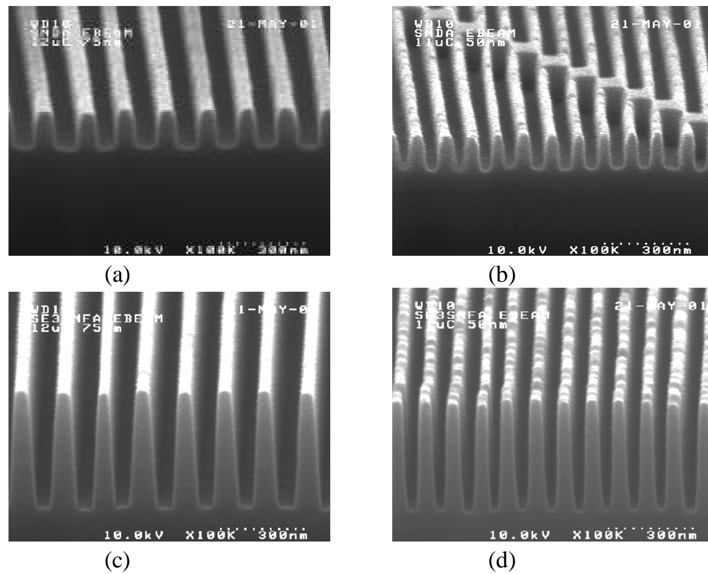

Figure 14. SEM images of 75nm (a) and 50nm (b) L/S patterns in 120nm thick ARC/hardmask material after the resist strip of KRS-XE. SEM images of 75nm 12 (c) and 50nm 12(d) L/S patterns etched into 300nm silicon dioxide layer using Si based ARC/hardmask material as an etch mask.

KRS-XE is a low activation energy resist that is insensitive to variation in post-exposure processing.[14, 22, 23] This material is based on a phenolic polymer backbone and thus has etch characteristics similar to those of conventional DUV positive photoresists. Electron beam exposure (11-13 $\mu C/cm^2$) was followed by a 30min delay and development. No post-exposure bake was used. Dense images as small as 50nm, the limit of the pattern generator program, were resolved.

Since substrate reflectivity and swing ratios are not at issue in electron beam lithography, the ARC properties of these materials are irrelevant for this application. However, for consistency, they will continue to be referred to as ARC/hardmasks. High image quality resist profiles were observed for 75nm and 50nm dense L/S features printed in KRS-XE resist at a film thickness of 110nm over ARC/hardmask layer. Chorine plasma chemistry was used to transfer the resist patterns into 120nm thick ACR/hardmask material. Figures 14a, 14b show the 75nm and 50nm features transferred into 120nm ARC/hardmask material after the resist strip. These images were used for subsequent patterning of 300nm of SiO_2 in highly polymerizing fluorocarbon-based plasma chemistry. Figures 14c, and 14d show the high resolution pattern transfer into a 300nm oxide layer attained by using ARC/hardmask materials as an etch mask. These images clearly demonstrate the utility of using a thin resist coupled with an ARC/hardmask for production of very high resolution, high aspect ration images for next generation device fabrication.

10. Conclusions

A novel Si based PECVD ARC/hardmask materials with excellent tunability of optical properties at 193 and 248nm have been developed. These materials allow the patterning of a variety of device features that would otherwise be challenging or impossible with conventional SLR schemes. The unique properties of these materials enable the design of graded ARCs with extremely high reflectivity control capabilities. Etch selectivity to ARC/hardmask to resist of 2.5:1 have been attained — values that significantly exceed those of organic ARC to resist. These materials also have inherent hardmask properties that provide superior etch resistance for dielectric stack patterning. Etch selectivity of >10:1 for ARC/hardmask to SiO_2 have been shown. Furthermore, ultra-high aspect ratio (>65:1) 120nm DT features in Si have been achieved with this ARC/hardmask technology. Potential extendibility of this approach to feature sizes below 100nm has been also evaluated. Resolution down 50nm was demonstrated followed by pattern transfer into SiO_2. This ARC/hardmask approach provides a complete imaging and etch solution for high resolution lithography and thus enables a thin resist process that will be essential for patterning with 157nm, EPL and EUV lithography as well as allowing the extension of 248 nm and 193 nm lithography using high NA systems.

Acknowledgements

The authors would like to thank Bob Lang for his excellent lithography process support. Dario Goldfarb, Matt Colburn and Colin Brodsky are thanked for the valuable discussions and contributions on image collapse issues. We are extremely grateful to Alessandro Callegari for providing simulation package based on Fresnel's algorithms as well as fruitful optics discussions. We would like for thank Kelly Garcia and Amber Jaffri for the SEM support. Finally, we also would like to acknowledge Wu-Song Huang for providing the polymer for the KRS-XE formulations and to James Bucchignano for the electron beam patterning.

REFERENCES

1. H. B. Cao, P. Nealey, and W. D. Domke, J. Vac. Sci. Technol. B **18** (6), 3303 (2000).
2. D. Goldfarb, J. de Pablo, P. Nealey, J. Simons, W. Moreau, M. Angelopoulos, J. Vac. Sci. Technol. **19**, 600 (2001).
3. M. Rothschild *et al.,* Photopolym. Sci. Technol. (Japan), **13**, 369 (2000)
4. Q. Lin, K. Petrillo, K. Babich *et al*., Proc. SPIE **3678**, 241 (1999).
5. M. K. Crawford *et al.,* Proc. SPIE, **3999**, 357 (2000).
6. T. Brunner, Proc. SPIE **1466**, 61 (1991).
7. E. Hecht and A. Zajac , Optics, (Wiley, 1979), pp. 312-314.
8. T. Tanaka, N. Asai, and S. I. Uchino, Proc. SPIE **2726,** 573 (1996).
9. K. Babich, A. Callegari, C. Jahnes , Proc. Photopolymers , 260 (1997).
10. M. Xu and T. M. Ko, J. Vac. Sci. Technol. B **18** (1), 127 (2000).
11. T. Brunner *Proc. SPIE, **4691** (2002)*
12. L. A. Joesten, M. Moynihan, T. Lindsay *et al*., Proc. SPIE **3333**, 960 (1998).
13. W. W. Lee, Q. He, G. Xing *et al*., IEEE Intl. Interconnect Tech. Conf., 84 (1998).
14. D.R. Medeiros J. Photopolym. Sci. Technol. **15**, 41 (2002)
15. A. Mahorowala *et al.,* J. Vac. Sci. Technol. A **18**(4), 411 (2000).
16. M. Armacost *et al.*, IBM J. Res. Develop. **43** (1/2), 39 (1999)
17. K. Babich unpublished results
18. T. Tanaka, M. Morigami, N. Atoda, Jpn. J. Appl. Phys., Part 1 **32**, 6059 (1993)
19. L. Qui, Y. B. Gianchandani, J. Vac. Sci. Technol. B **18(6)**, 3450 (2000).
20. A. Kawai, T. Abe, Jpn. Photopolym. Sci. Technol. **14**, 515 (2001)
21. C. J. van Oss, R. J. Chaudry, M. K. Goode, Langmuir **4**, 884 (1988)
22. R. Kwong, W-S. Huang, W. Moreau, R. Lang, C. Robinson, D. R. Medeiros, A. Aviram, R. C. Guarnieri, M. Angelopulos, Mater. Res. Soc. Symp. Proc. **584**, 147 (2000).
23. D. R. Medeiros, W. M. Moreau, K. Petrillo, M. Chauhan, W-S. Huang, C. Magg, D. Goldfarb, M. Angelopoulos, P. Nealey Proc. SPIE, **4345**, 421 (2001).